1 AGENCY USE ONLY (Leave blank)	2 REPORT DATE	3 REPORT TYPE AND DATES COVERED
	May 1991	professional paper

4 TITLE AND SUBTITLE

LASER-BASED DISPLAY TECHNOLOGY DEVELOPMENT AT THE NAVAL OCEAN SYSTEMS CENTER (NOSC)

5 FUNDING NUMBERS

PR: CDB2
WU: DN306242
PE: 0602232N

6 AUTHOR(S)

T. Phillips, J. Trias, M. Basher, P. Poirier, W. Dahlke, and W. Robinson

7 PERFORMING ORGANIZATION NAME(S) AND ADDRESS(ES)

Naval Ocean Systems Center
San Diego, CA 92152-5000

8 PERFORMING ORGANIZATION REPORT NUMBER

9 SPONSORING/MONITORING AGENCY NAME(S) AND ADDRESS(ES)

Naval Ocean Systems Center
Block Programs
San Diego, CA 92152-5000

10 SPONSORING/MONITORING AGENCY REPORT NUMBER

11 SUPPLEMENTARY NOTES

12a DISTRIBUTION/AVAILABILITY STATEMENT

Approved for public release; distribution is unlimited.

12b DISTRIBUTION CODE

13 ABSTRACT (Maximum 200 words)

For several years, the Naval Ocean Systems Center (NOSC) has been working on the development of laser-based display systems with the goal of upgrading the image quality and ruggedness of shipboard displays. In this paper we report work on our major task of developing a full-color laser-addressed liquid crystal light valve (LCLV) projection system.

Published in *SPIE/SPSE Proceedings*, vol. 1454, Feb 1991.

14 SUBJECT TERMS		15 NUMBER OF PAGES
data compression data fusion workstation	displays data quality data retrieval	16 PRICE CODE

17 SECURITY CLASSIFICATION OF REPORT	18 SECURITY CLASSIFICATION OF THIS PAGE	19 SECURITY CLASSIFICATION OF ABSTRACT	20 LIMITATION OF ABSTRACT
UNCLASSIFIED	UNCLASSIFIED	UNCLASSIFIED	SAME AS PAPER

21a NAME OF RESPONSIBLE INDIVIDUAL	21b TELEPHONE (*Include Area Code*)	21c OFFICE SYMBOL
T. E. Phillips	(619) 553-3596	Code 414

LASER-BASED DISPLAY TECHNOLOGY DEVELOPMENT AT THE NAVAL OCEAN SYSTEMS CENTER (NOSC)

Thomas Phillips, John Trias, Mark Lasher, Peter Poirier, Weldon Dahlke, and Waldo Robinson
Naval Ocean Systems Center
San Diego, CA, USA

ABSTRACT

For several years, the Naval Ocean Systems Center (NOSC) has been working on the development of laser-based display systems with the goal of upgrading the image quality and ruggedness of shipboard displays. In this paper we report work on our major task of developing a full-color laser-addressed liquid crystal light valve (LCLV) projection system.

1.0 INTRODUCTION

An all solid-state 1075-line laser raster scanner system with a limiting resolution greater than 1300 TV lines and full-color capability has been developed. The laser raster scanner (LRS), designed with acousto-optic devices for both vertical and horizontal deflection, is used in conjunction with a polarization switching scheme to photoactivate three liquid-crystal light valves (LCLV) for video-rate full color large screen projection display. The LRS was designed to interface with a 1075-scan-line, 2:1 interlace format with 1280 (H) by 1024 (V) active pixels conforming to a modified EIA RS-343A TV Standard to satisfy the Navy shipboard Digital Television Generator (DITEG) display format.[1]

The project described here is the main component of a set of laser-based display tasks in progress at NOSC for which the primary goal is to enhance the capability and ruggedness of shipboard displays. The objective of this task is to develop and demonstrate a prototype color display projector with high resolution, brightness, and constrast using laser-addressed LCLVs.

1.1 Background

The display group at NOSC has an ongoing task of looking for ways to improve the resolution of CRT-addressed LCLV shipboard projectors. In an attempt to fully utilize the resolution of LCLVs, an investigation was begun into the feasibility of using scanned laser beams as an addressing mechanism to replace the CRT. Initial efforts using the laser-addressed approach incorporated rotating mirror/galvanometer, acousto-optic/galvanometer, and finally all-acousto-optic deflection systems.

Monochrome prototypes utilizing conventional AO deflection techniques were tested at standard 525-line rates and found to be useful in addressing the LCLVs. In order to achieve the higher 1000-line resolution, the acoustic traveling chirp lens approach was employed.[2,3] The original prototype design for our laser scanner was produced by Chesapeake Laser Systems, who delivered a single-channel scanner in 1987. The current system has taken this basic design approach and modified it to improve throughput efficiency and resolution, and allow for full color operation.

1.2 Overall System Description

The major components of the LRS color system are the laser, raster scanner, polarization multiplexing switches, LCLVs, projection optics and an arc lamp. Figure 1 shows a schematic of the prototype incorporating the LRS in a large-area projection-display system.

The projector can be conveniently divided into two basic subunits which operate on opposite sides of the light valves. The first is the input subsystem, consisting of the laser, raster scan optics, multiplexing optics, and associated drive electronics. The second is the output subsystem, consisting of the light valves, projection lamp, relay optics, liquid-filled polarizing beamsplitter, color separation filters, compensation plates, and projection lens. In our prototype, these two subsystems are stacked on top of each other to form a very compact, large-screen, color projection system.

The present LRS uses three Hughes light valves with cadmium sulfide photoconductors. Red, green, and blue video information is time multiplexed onto these light valves and a 400-watt xenon arc-lamp is used to readout this information

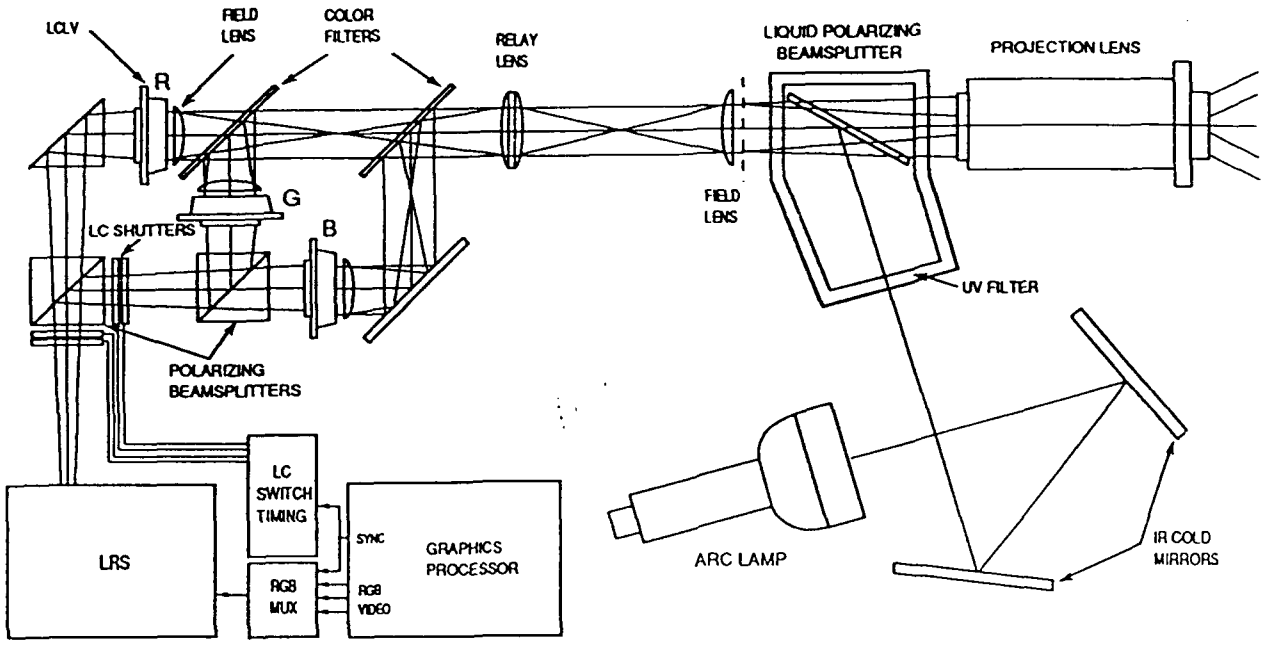

Figure 1 Color Laser-Addressed Light Valve Display System

and project to a 5 foot diagonal square image. The following sections describe the basic design parameters of the LRS, the characteristics of the major components, and the performance of the prototype display system.

2.0 LASER SCANNING SYSTEM

2.1 Acousto-Optic Deflection

The primary constraint upon the design of the LRS was the 1075-line RS-343A input signal format. As shown in Table 1, this defines the total horizontal line time, T, to be 31 μsec, of which 7 μsec is blanked for horizontal flyback.

If a standard acousto-optic deflector is used to produce the horizontal scan, the number of resolvable spots, N, for such a device can be approximated by.[4]

$$N = \tau \, \Delta f \left[\frac{T-\tau}{T} \right] \qquad (1)$$

where τ is the time for acoustic wave to transit the optical beam (access time), Δf is the bandwidth of frequency sweep, and T is the time during which frequency sweep occurs.

With the RS-343A format the scan output must be active for 24 out of 31 μsec. This means the access time must be no greater than 7 μsec. Likewise, the frequency sweep can occur over no more than the total line time, giving T = 31 μsec. The requirement for N = 1280 resolvable spots/line therefore indicates the need for a frequency bandwidth of Δf = 236 MHz. Combining this with the necessity of preventing overlap between the first and second diffraction orders, results in required operation in the range of 236 to 472 MHz. Design of a TeO_2 deflector capable of maintaining uniform Bragg diffraction efficiency across this frequency range is difficult. However, due to the high acoustic figure of merit for scanning applications in the visible region, as well as commercial availability, TeO_2 is still the best material available for this type of deflection system.

To overcome these difficult bandwidth requirements, a traveling-lens type AO scanner was used. This technique utilizes the principle that an acoustic chirp (linear frequency sweep) causes light to converge or diverge like a cylindrical lens. If a short-

TABLE 1. LRS Video Characteristics, RS343-A		
Raster Format	1075	lines
Active Line Time	24	µsec
Horizontal Blanking Time	7	µsec
Total Horizontal Line Time	31	µsec
Frame Rate	30	Hz (2:1 interlace)
Timing and Levels scaled from RS343-A TV Standard		

duration chirp (5-10 µs) is produced and allowed to propagate across an illuminated aperture, the effect is to scan a focused spot along a line during the transit time of the AO cell (Figure 2). The resolution of a traveling lens scanner is related to the active line time rather than the acoustic access time. The total number of resolvable elements in this case can be approximated by [5]

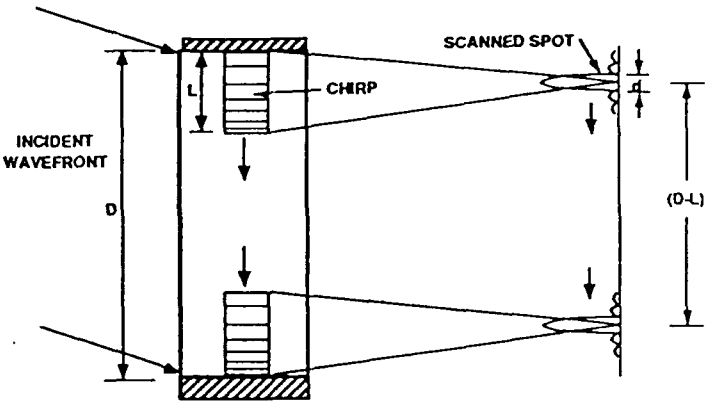

Figure 2 Acoustic Chirp Scanning

$$N = \Delta f \; t_{active}. \qquad (2)$$

Using this method with the RS-343A active-line time, and N = 1280, we have

$$\Delta f = 1280/24 \; \mu sec = 53.3 \; MHz. \qquad (3)$$

Thus, the traveling chirp lens approach allows one to achieve the desired resolution using acoustic frequencies in the 50 to 100 MHz range, which are much better suited for flat response in TeO_2 crystals.

Flooding the entire aperture of the acoustic crystal through which the chirp travels would waste much of the available laser energy. To achieve greater optical efficiency, a low-resolution 'tracker' acoustic cell precedes the traveling wave lens in our system. The tracker provides a scanned beam that matches the physical width of the chirp lens and follows the traveling chirp as it propagates across the aperture.

In the vertical direction, the sweep is much slower, allowing use of standard AO deflection techniques. In this case, $T >> \tau$, and equation (1) reduces to:

$$N = \tau \, \Delta f. \qquad (4)$$

For a resolution of 1024 lines with a 50MHz bandwidth we need τ = 20.5 µsec. As seen in Table 1, the vertical blanking interval is more than adequate to accomodate this access time.

2.2 Optical System

Using the traveling wave lens technique as a basis, a 1280 horizontal by 1024 vertical resolution video raster scanner was developed using four AO cells (see Figure 3).[5] The output of this scanner was then used as the image source for the sequential color scheme described below.

A diode laser-pumped Nd:YAG, doubled to 532nm (18mW, 40:1 polarization ratio), is used as the cw laser source. Its output is focused by lens L1 to a 85µm spot within the acoustic field of the first AO cell. This cell, a longitudinal mode TeO_2 device (CTI Model 3200) operating at a carrier frequency of 200 MHz, provides the laser video modulation.

Light from the modulator is re-collimated by L2, circularly polarized, and sent through the tracker cell. This cell is a shear mode TeO_2 scanner (CTI Model 4075) which sweeps from 50 to 100 MHz in 24 µsec to provide a coarse scan to 'track' the chirp cell's traveling acoustic lens. Beyond the tracker, an anamorphic cylindrical lens pair, L3x and L3y, work together with the spherical L4 to provide the desired beam shape for input to the chirp cell. The combination of tracker and chirp AO

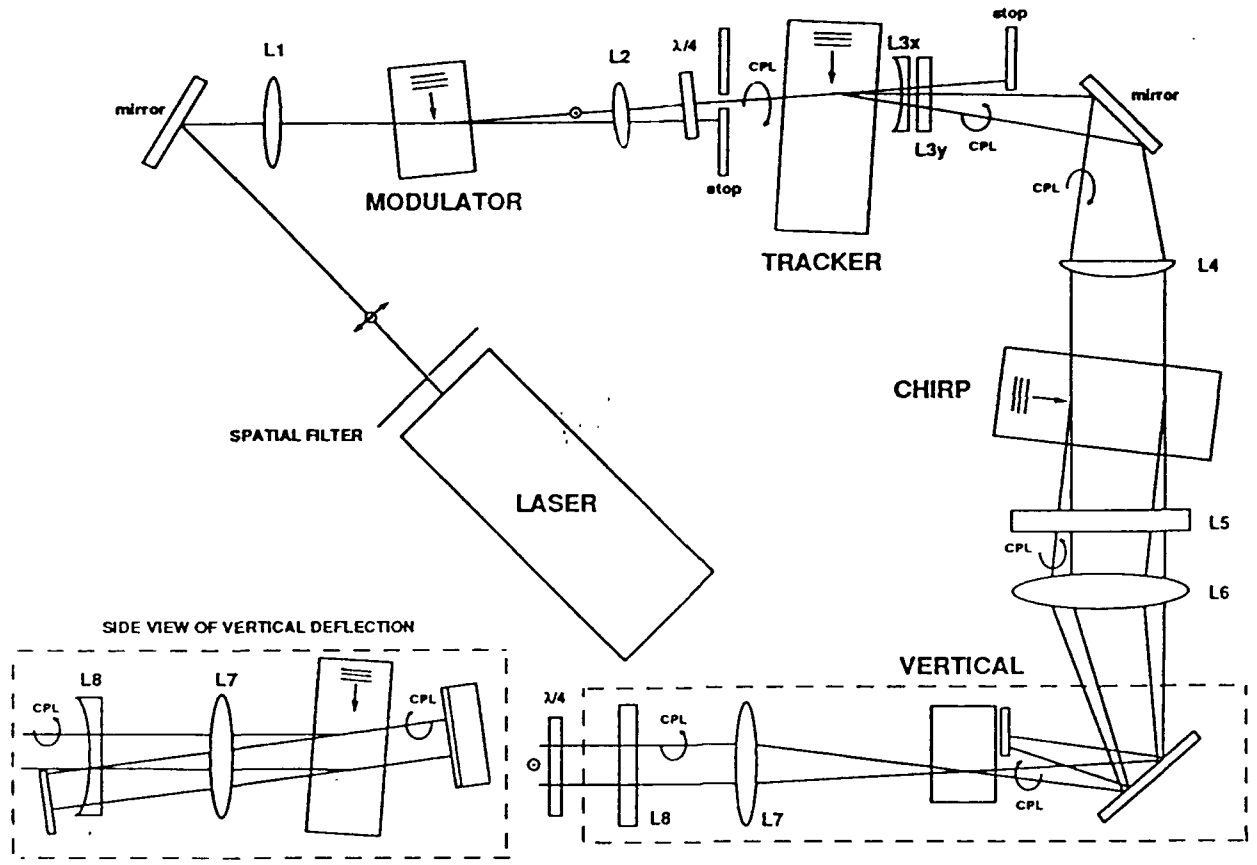

Figure 3 Optical Layout of Laser Raster Scanner

cells constitutes the X-scan of the LRS (24 μsec active time, 7 μsec blanking time).

To achieve the desired vertical resolution, the beam must be expanded in the y-direction at the y-deflector. Lens L5 (cylindrical) and L6a/b (a pair of spherical doublets) provide this expansion. In addition, L6 operates in the x-direction as a field lens to redirect the beam through the y-deflector. This deflector, also a shear-wave TeO_2 device, sweeps from 50 to 100 MHz during the vertical field time of 16.7 msec.

The final imaging elements in the LRS are lenses L7 (spherical doublet) and L8 (cylindrical). These accept the two-dimensionally scanned beam and produce the laser image which illuminates the light valve photoconductors. After passing through L7 and L8, the final video image is converted to linear polarization with a quarter-wave plate in preparation for the RGB-multiplexing polarization switches described below.

Since all three scanning elements are shear mode TeO_2 devices, they operate most efficiently with circularly polarized light (CPL).[6] For best bandwidth, the input polarization at each must also be of the correct sense of rotation. Unfortunately, the shear mode output has a polarization opposite to the input. This problem can be conveniently remedied by folding the system as indicated in Figure 3. In addition to producing a more compact system, each mirror reverses the polarization sense of the CPL, providing proper polarization for the following deflector.

2.3 RGB Multiplexing Switches

The key to the NOSC color scheme is the sequential redirection of the output of a single scanner, allowing it to address all three light valves. In this way one can produce three images that are more nearly identical than could be obtained with separate scanners. This was accomplished through the use of liquid crystal (LC) polarization switches.[7] Their function in this case is to rotate the polarization of the scanned laser image by either 0 or 90 degrees, and exploit the beam steering

capabilities of polarizing beamsplitters to direct the image field to the proper light valve.

Figure 1 shows the location of the switches in the LRS system. Note that each switch location actually consists of a pair of two individual switches. This was done to achieve the necessary fall time required by the LRS to avoid overlapping of the RGB fields. Although these devices have a short rise time, their decay time (~1 msec) is too long to accomplish switching during the 790 µsec vertical retrace between video fields. By using two switches in tandem one can compensate for the relatively slow relaxation time from the first switch by biasing the second switch to relax in an equal, but opposite, polarization rotation sense.[7] Using this scheme, fall times of less than 100 µsec are possible.

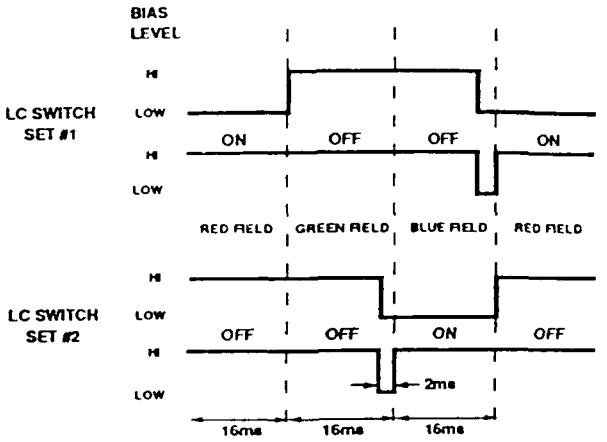

Figure 4 Polarization Switch Timing

The timing diagram in Figure 4 shows the sequencing of control signals to the two sets of switches. Whenever both switches in a set are at the same voltage (both HI, or both LOW) there is no net effect on the transmitted polarization state of the light. This is defined as the 'OFF' state in the diagram. If the two switches in a set are at different voltages then the transmitted image has its polarization rotated by 90 degrees. This is defined as the 'ON' state of the switch pair.

The image coming from the last quarter-wave plate in the scanner is vertically polarized. To direct the red video field onto the appropriate light valve photoconductor, switch #1 is turned 'ON', resulting in transmission through the first beamsplitter and illumination of the red LCLV (independent of the state of switch #2). For the green video field, both switches are left in the 'OFF' state, and the image reflects off of both beamsplitters. For the blue video field, switch #2 is turned 'ON' to permit transmission through the second beamsplitter to the blue LCLV, thus completing one complete "field" of RGB video. Although the field rate for each color is one third that of the source RGB video, the persistence of the CdS light valves is sufficient to avoid flicker problems in this sequencing process.

3.0 OUTPUT PROJECTION SYSTEM

3.1 Liquid Crystal Light Valve

The most significant characteristic that sets our projector apart from most laser scan systems is the use of liquid crystal light valves as image converters. The LCLV, a multilayer thin film device which operates in a reflective mode, allows conversion of the relatively low power laser input image into a high-power arc lamp-based output image. In addition, it allows generation of a projected image whose color is independent of the color of the laser image source.

Figure 5 shows the structure of the Hughes LCLVs used in our current system.[8] Their operation is based upon use of a CdS photoconductor to photoelectrically switch voltage across a liquid crystal material. On the input side, laser light in the form of a two-dimensional raster image illuminates the photoconductor, significantly lowering its impedence. As a result, most of the bias voltage applied across the multilayer sandwich will switch from the initially high-impedence CdS to the liquid crystal layer, thus changing its birefringent properties. The change is proportional to the incident laser light intensity.

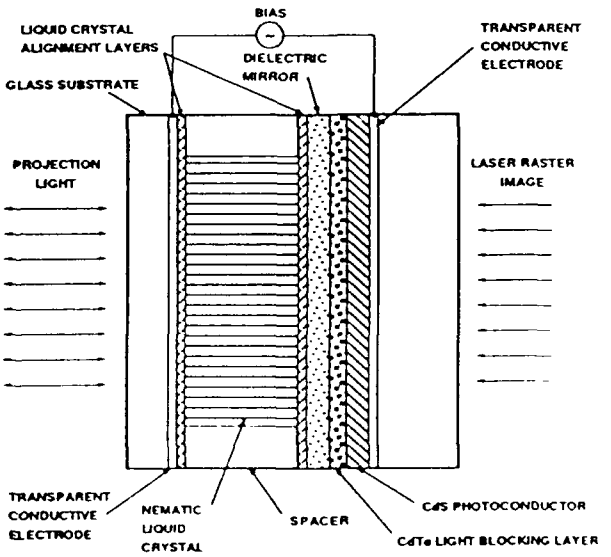

Figure 5 LCLV Cross Section

On the output side, the high-intensity polarized projection light is spatially modulated by the birefringence pattern in the liquid crystal. This light is then reflected back through a polarization-sensitive beamsplitter which provides the intensity modulation for the final projected image.

The LCLV characteristics that are critical in this LRS display include spectral response, input sensitivity, resolution and speed. Typical values for the devices we've tested, which were fabricated for display applications, are given in Table 2. The sensitivity, resolution, and speed given in the table are nominal values which are valid when the devices are operated at the optimum bias voltage and frequency range.

TABLE 2. LCLV Characteristics

Active Area	50 mm diameter
Spectral Response	500-550 nm
Sensitivity	50-100 $\mu W/cm^2$
Output Resolution (50% MTF, white)	15-20 lp/mm
Rise Time	~100-400 msec
Fall Time	~100-400 msec
Preferred Bias Voltage	10 V
Preferred Bias Frequency	10 KHz

The CdS photoconductor has a spectral response which peaks around 520 nm, making it useful for either the 514 nm argon line or the 532 nm line of doubled Nd:YAG. The input sensitivity of 50-100 $\mu W/cm^2$ represents a time-averaged value to achieve response saturation. The LCLVs exhibit no reciprocity failure at the pixel rates used in our raster video system (a potential problem with persistence-free laser images).

The resolution of LCLVs depends upon the spectral bandwidth and polarization quality of the output light, as well as the bias voltage and frequency. For display applications, white light from an arc lamp is typically used, and polarization is accomplished via polarizing beamsplitter prisms. The resolution values listed are representative of this application for the LCLVs in our system.

3.2 Projection Optics

Since the LRS projector was targeted for short-throw shipboard applications, its output design was based on the single-projection-lens configuration shown in Figure 1. It consists of three LCLVs, a xenon arc lamp, a fluid-filled polarizing beamsplitter prism, infrared, ultraviolet and color separation filters, a relay lens, field lenses, and a projection lens.

In order to reduce the amount of design effort, the projection lens, polarizing prism, and arc lamp assembly were taken as a whole unit from a Hughes monochrome light-valve projector. In order to provide this subunit with the required input image, a relay lens was included to overlap the three LCLV images at a single image plane. This also provides sufficient space to include color separation filters in the optical path. Field lenses were included at each light valve and near the intermediate image plane to assure the proper telecentric input at the LCLVs.

4.0 PROTOTYPE SYSTEM PERFORMANCE

4.1 Acousto-Optic Devices

In order to assure optimum use of our particular acousto-optic devices, we observed the acoustic field inside each crystal using schlieren imaging. The usable height of the acoustic beam was found to be about 2mm, which prompted a redesign of some of the original scanner optics. Providing a narrower beam at the input to the AO deflectors resulted in improved throughput efficiency. These experiments also showed that significant acoustic sidelobe generation begins to occur at about 500 mW of RF drive power, which can lead to spatial noise in the output image if the input beam diameter is not kept within 2mm.

The focused chirped pulses were also observed using the schlieren technique. By strobing the laser light, individual pulses (20nsec), representing approximately one pixel duration, were observed.

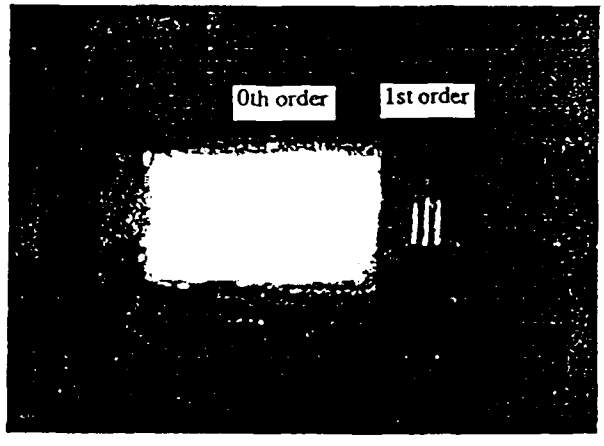

Figure 6 Acousto-Optics Chirp Focusing

Figure 6 shows a burst of 3 pulses. The chirp signal used in the LRS is digitally synthesized from a ROM chip containing a special aperiodic sequence of pulses which contain the necessary frequencies for the 6μsec, 50-100MHz FM ramp.

4.2 Liquid Crystal Shutters

The liquid crystal shutters were Tektronix pi-cells fabricated for the Tektronix color shutters.[7] We removed the laminated polarizers and provided the necessary signals for RGB multiplexing. When used in tandem in the push-pull format mentioned in section 2.3, we were able to achieve rise and fall times of about 50 μsec and 80 μsec, respectively. Overall transmittance through each uncoated cell was about 90%, or 81% per pair. In future designs, these could be cemented together (and cemented to the beamsplitter cubes) to minimize optical losses. When used with wide band polarizing beamsplitter cubes, the extinction ratio was about 45:1.

4.3 Laser Scanner

Developing scanners of this complexity and resolution requires precise knowledge of the laser beam size, polarization, and convergence at all points in the system. Unfortunately, PC-level software to do this was not readily available. Consequently, we generated ray-trace software tools to model the acousto-optic devices (modeled as variable-frequency gratings) and Gaussian beam propagation through the system.[9] This allowed much better predictive capability when compared to non-Gaussian traces performed with standard ray-trace software, particularly with regard to lens placement and beam diameter.

The last two lenses in the scanner proved to have the greatest impact on image aberrations. Initial designs used a single, off-the-shelf achromat for L7. This produced a good image on axis, but exhibited a great deal of the typical off-axis aberrations. As a first step toward reducing this problem, a new L7 doublet lens was designed which, when used with a longer L8 cylinder focal length, would produce the desired image aspect ratio and achieve improved resolution throughout the image field. Figure 7 shows a predicted spot diagram for different locations in the image plane, showing the difference between the original +70mm achromat and the custom doublet now being used.

Our current test equipment is inadequate to measure the modulation at full addressability at the 40 mm by 30 mm image plane, or to measure optical aberrations. When driven with an on-off video pattern at full 1280-pixel resolution, the axial LRS image plane exhibits good modulation. Off-axis modulation, while much improved by the addition of new lenses L7 and L8, is at the limit of visibility. Improvements in this area can be made by utilizing more sophisticated output lens designs.

The main drawback to the use of four AO cells in the LRS is in the overall throughput efficiency. Measurements of the multiplexed image at the input surface of the light valves showed power levels on the order of about 1mW (2.4mW/cm^2). From the data shown below, it would appear that at least a 10-fold increase in photoconductor irradiance is necessary to operate at full addressability with an MTF of 0.5 or higher.

4.4 Doubled-YAG Laser

Generally, the diode-pumped doubled Nd:YAG lasers have operated admirably while significantly reducing system size and input power over earlier argon-based designs. Early prototype lasers exhibited some long-term amplitude stability problems, but devices now available show promise toward solving this problem.

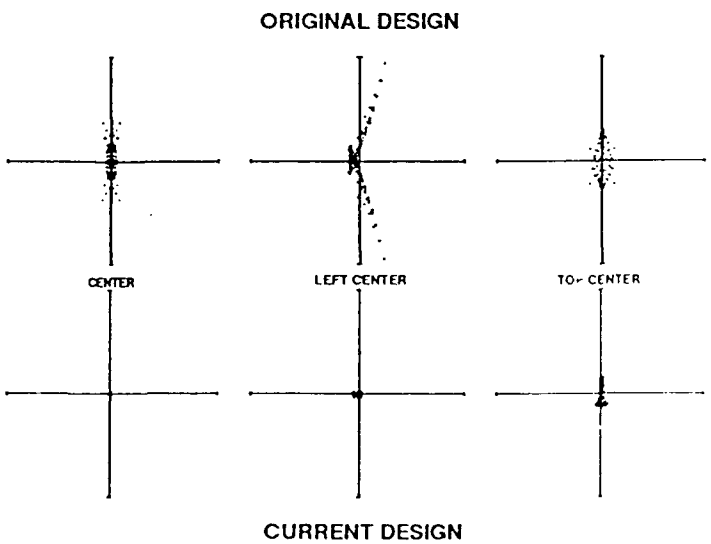

Figure 7 Calculated Spot Diagrams for L7/L8 Lens Pair
(Axes: ±0.5mm)

A word of caution is in order for potential users of these lasers, however. The particular laser used for much of our recent work did have two extremely frustrating problems relating to the optical characteristics of its output: it was neither TEM_{oo} nor monochromatic. The output beam was a mixture of higher-order modes, which resulted in reduced image quality due to effects on modulator bandwidth[10] and deflector spot size, as well as large variations from Gaussian predictions in beam divergence[11] throughout the system. The polychromaticity also had major impact on image resolution. In addition to the expected line at 532 nm, a significant line (~ 20% power) existed at 534 nm. The secondary line produced a distinct ghost image which was separated from the primary image by about 5-6 pixels. Newer versions of the laser are proving to be much improved in both of these respects.

4.5 Light Valve Performance

To determine the effect of limited laser power on our system, modulation measurements were made on the LCLVs at various spatial frequencies as a function of input power. A Michelson interferometer was used to write sinusoidal gratings onto the CdS photoconductor. Readout of the fringe patterns was made in white light using a scanning slit beam profiler. Fringe spacing could be easily and accurately changed by tilting one arm of the interferometer, calibration being performed using an Air Force test chart.

Figure 8 shows a comparison of the specific light valves used in the current LRS system for one spatial frequency. The data were taken at 10 lp/mm, at two different bias frequencies (500 Hz and 10 KHz). Note the rapid decay of modulation in the 10 KHz data as the input illumination power is lowered. Lowering the drive frequency to 500 Hz provides improved modulation at very low input levels for two of the light valves, but much lower modulation overall. It is apparent that operation at the limited input levels now available in our scanner will have adverse effects on system resolution.

4.6 Projector Output

Full color renditions of graphic images have been demonstrated using the multiplexed LCLV approach, though enhancements to the output portion of our projector have only recently begun. Using a single 400 W xenon arc lamp, the present white illuminance on a 42 inch square screen is in the 2-5 ft-C range. Alternating white and black lines at full resolution are visible at the screen center, though we still have some problems to solve with regard to RGB convergence throughout the image. Currently, the CdS provides sufficient image retention to avoid flicker problems with our multiplexing process. Off-the-shelf color separation filters provide reasonable color rendition, though trimming would be necessary in final designs (particularly in the blue).

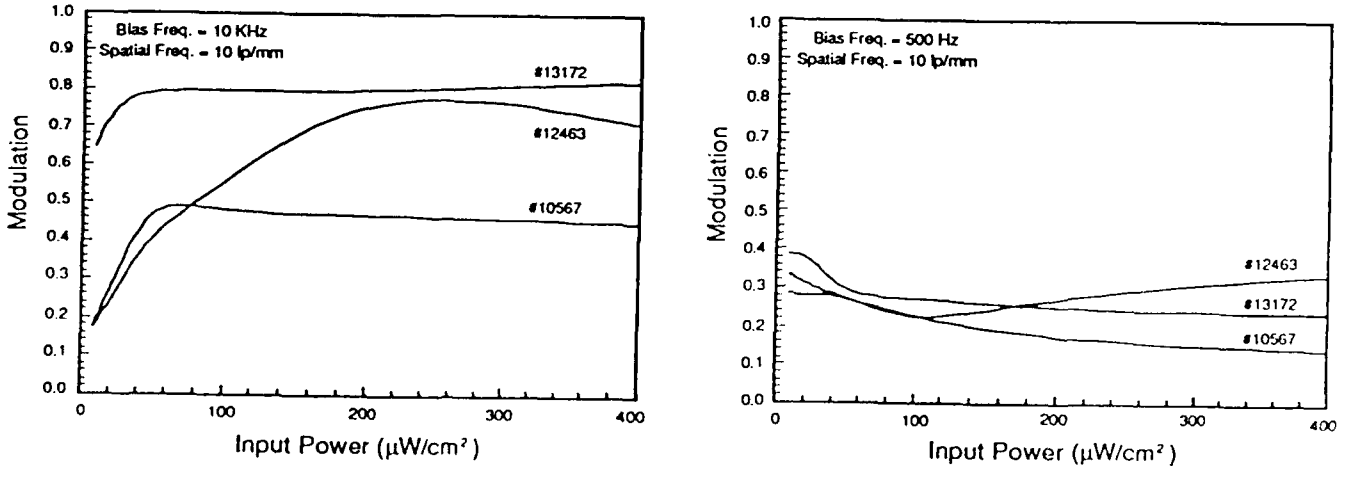

Figure 8 Modulation data for lightvalves used the LRS for two different bias frequencies.

5.0 CONCLUSION

The work done to date on our prototype scanner indicates that a compact, high-resolution color projector could be developed based upon the laser addressing of liquid crystal light valves. The traveling lens and tracker combination shows potential for very high resolution, and the sequential addressing of RGB light valves holds promise for easing the convergence problems inherent in high-resolution projection displays.

Questions remain, primarily in the area of efficiency, manufacturability, and cost. The 2% throughput efficiency of the LRS, combined with the 3:1 multiplexing, and the light valve's 50 $\mu W/cm^2$ input power requirements, indicate that at least a 10-fold increase in optical power is needed. The input and output systems are very complex optically, so convergence is achieved at the cost of generating alignment complexity. Much work is needed in the area of optical and optomechanical designs that will relax the very tight tolerances required for good convergence of high-resolution images. Finally, the current cost of light valves and acousto-optic devices will limit this technique to the high-end market.

Looking to the future, one could anticipate immediate improvements to resolution by increasing the active line from 24 µsec to the full 31 µsec available (a 30% increase), refining the optical design of the output scan lenses so that the system is AO-limited, and increasing the optical power to the light valves. More involved enhancements are also being considered. Multiple-beam scanners could be implemented with only moderate modifications to the basic design. Improvements to the bandwidth capabilities of the acousto-optic devices themselves would produce proportional improvements to system resolution.

Finally, transition of this technique to the newer light valves based on silicon photoconductors looks promising. These devices, which have faster response times and better resolution characteristics than their CdS counterparts, exhibit peak sensitivity in the near-IR. This would allow LRS designs which incorporate high-efficiency directly modulatable laser diode sources. If the alignment process can be simplified and proposed work on the above enhancements is successful, we anticipate that the technology described will result in demonstration of projectors in the 2000-line video range.

6.0 ACKNOWLEDGEMENTS

The authors wish to express their appreciation to Dr. Sherman Gee of the Office of Naval Technology and Commander K. Paige of the AEGIS program office NAVSEA PMO-400 for their encouragement and continued support. We would also like to thank the Industrial Products Division of Hughes Aircraft for the generous loan of several liquid crystal light valves.

7.0 REFERENCES

1. SHIPS-D-5968A, Appendix Q 1 AUG 89.
2. Foster, L.C., et al, "A High-Resolution Linear Optical Scanner Using a Traveling-Wave Acoustic Lens", Applied Optics, Vol. 9, No. 9, pp 2154-2160, 1970.
3. Merry, J.B., and Bademian, L., "Acousto-Optic Laser Scanning", Proc. SPIE Vol. 169, pp 56-59, 1979.
4. Bademian, L., "Acousto-optic laser recording", Opt. Eng., Vol 20, No. 1, pp 143-149, 1981.
5. Trias, John, et al, "A 1075-Line Video-Rate Laser-Addressed Liquid-Crystal Light-Valve Projection Display", Proc. S.I.D., Vol 29/4, pp 275-277, 1988.
6. Uchida, Naoya,"Optical Properties of Single-Crystal Paratellurite (TeO2)",Phys.Rev.B,Vol.4,No.10, pp 3736-3745,1971.
7. Haven, T.J., "A liquid-crystal video stereoscope with high extinction ratios, a 28% transmission state, and one-hundred microsecond switching", Proc. SPIE Vol.761, pp 23-26, 1987.
8. Bleha, W.P., et al, "Application of the Liquid Crystal Light Valve to Real-Time Optical Data Processing", Opt.Eng., Vol.17, No.4, pp 371-384, 1978.
9. Herloski, R., et al, "Gaussian beam ray-equivalent modeling and optical design", App.Opt., Vol.22, No.8, pp 1168-1174, 1983.
10. Lucero, J.A., et al, "Effect of Laser Beam Transverse Mode and Polarization Properties on Acousto-Optic Modulator Performance", Proc. SPIE Vol. 90, pp 32-39, 1976.
11. Luxon, J.T., et al, "Waist location and Rayleigh range for higher-order mode laser beams", App.Opt., Vol.23, No.13, pp 2088-2090, 1984.